



Original Research Paper

## Pyrolysis of low-value waste sawdust over low-cost catalysts: physicochemical characterization of pyrolytic oil and value-added biochar

Ranjeet Kumar Mishra<sup>1</sup>, Kaustubha Mohanty<sup>2,\*</sup>

<sup>1</sup>Department of Chemical Engineering, M.S. Ramaiah Institute of Technology, 560054 Bangalore Karnataka, India.

<sup>2</sup>Department of Chemical Engineering, Indian Institute of Technology Guwahati, 781029 Assam, India.

### HIGHLIGHTS

- Effect of CaO, CuO, and Al<sub>2</sub>O<sub>3</sub> catalysts on yield and properties of Sal wood sawdust's pyrolytic oil investigated.
- Using catalysts increased the carbon content and heating value, and reduced the viscosity of the fuel.
- Using catalysts increased the hydrocarbons and reduced the acids and phenols contents.
- The characteristics of the obtained biochar revealed its suitability for extensive industrial applications.

### GRAPHICAL ABSTRACT

### ARTICLE INFO

#### Article history:

Received 12 August 2022

Received in revised form 30 September 2022

Accepted 13 November 2022

Published 1 December 2022

#### Keywords:

Sal wood sawdust  
Pyrolysis  
Low-cost catalyst  
Biochar  
Pyrolytic oil

### ABSTRACT

The present work deals with an experimental investigation into the generation and characterization of pyrolytic oil and biochar from Sal wood sawdust (SW). The pyrolysis experiment was performed in a semi-batch reactor at 500 °C and 80 °C/min heating rate with CaO, CuO, and Al<sub>2</sub>O<sub>3</sub> catalysts. Further, the pyrolytic oil and biochar were investigated using different analyses, including proximate analysis, elemental analysis, thermal stability, GC-MS, FTIR, field emission scanning electron microscopy, electrical conductivity analysis, higher heating value (HHV), zeta potential analysis, and ash content analysis. Pyrolysis results revealed that compared to thermal pyrolysis (46.02 wt%), the pyrolytic oil yield was improved by catalytic pyrolysis with CaO and CuO (50.02 and 48.23 wt%, respectively). Further, the characterization of pyrolytic oil revealed that the loading of catalysts considerably improved the oil's properties by lowering its viscosity (69.50 to 22 cSt), ash content (0.26 to 0.11 wt%), and oxygen content (28.32 to 16.60 %) while raising its acidity (4.2 to 9.6), heating value (25.66 to 36.09 MJ/kg), and carbon content (61.79 to 74.28%). According to the FTIR analysis, the pyrolytic oil contained hydrocarbons, phenols, aromatics, alcohols, and oxygenated compounds. Additionally, the GC-MS analysis showed that catalysts significantly reduced oxygenated fractions, phenols (20.23 to 15.26%), acids (12.23 to 6.56%), and increased hydrocarbons (12 to 16 wt%). Additionally, the results of the biochar analysis demonstrated that SW biochar was appropriate for a range of industrial applications, including in catalysts, supercapacitors, fuel cells, and bio-composite materials.

© 2022 BRTeam. All rights reserved.

\* Corresponding author at:  
E-mail address: [kmohanty@iitg.ac.in](mailto:kmohanty@iitg.ac.in)

## Contents

1. Introduction.....	1737
2. Materials and Methods.....	1738
2.1. Sample collection and preparation.....	1738
2.2. Characterization of fresh and calcined catalysts.....	1738
2.3. Physicochemical study.....	1738
2.4. Thermal stability analysis.....	1738
2.5 FTIR analysis.....	1738
2.6. Process parameter optimization.....	1738
2.7. Pyrolysis setup and experiments.....	1738
2.8. Characterization of pyrolytic oil.....	1739
2.9. GC-MS analysis.....	1739
2.10. Characterization of biochar.....	1739
3. Results and Discussion.....	1740
3.1. Characterization of catalysts.....	1740
3.2. Physicochemical characterization.....	1740
3.3. Thermal stability analysis.....	1742
3.4. Effect of temperature and heating rate on pyrolysis products yield.....	1742
3.5. Effect of catalysts on pyrolytic products yields.....	1744
3.6. Characterization of pyrolytic oil.....	1744
3.7. FTIR analysis of pyrolytic oil.....	1744
3.8. GC-MS analysis of pyrolytic oil.....	1745
3.9. Characterization of biochar.....	1746
3.10. Thermal stability, FTIR, and FESEM analysis of biochar.....	1747
4. Conclusions and Prospects.....	1747
Acknowledgements.....	1748
References.....	1748

### Abbreviations

Al <sub>2</sub> O <sub>3</sub>	Aluminum oxide
BET	Brunauer, Emmett, and Teller
CaO	Calcium oxide
CuO	Copper oxide
DTG	Derivative thermogravimetric
FESEM	Field emission scanning electron microscopy
FTIR	Fourier-transform infrared spectroscopy
GC-MS	Gas chromatograph-mass spectrometry
GHG	Greenhouse gas
HHV	Higher heating value
PCAH	Polycyclic aromatics hydrocarbons
SW	Sal wood sawdust
SWC	Sal wood sawdust biochar
TGA	Thermogravimetric analysis
VKD	Van-Krevelen diagram
ZP	Zeta potential

## 1. Introduction

The detrimental environmental impact of widespread fossil fuel utilization, and the growing political commitment to sustainable energy, have stepped up research into developing green fuels and alternate energy sources. According to the figures provided by the International Energy Agency (IEA), between 2007 and 2030, total energy consumption will rise from 12,000 to 16,800 Mtoe (million tonnes of oil equivalent) at a rate of 1.5% annually (Siddiqi et al., 2020). On the other hand, fossil fuels (coal, petroleum, etc.) are still the primary energy source, largely contributing to greenhouse gas (GHG) emissions and their consequences, i.e., global warming and climate change. According to the Intergovernmental Panel on Climate Change (IPCC) estimations, fossil fuel-related GHGs represent 56.6% of global GHG emissions (Siddiqi et al., 2020). In light of that, the UN Climate Panel's target is to reduce 50-80% of such GHGs by 2050 (Siddiqi et al., 2020). Reducing the dependency on fossil fuels and shifting expeditiously to renewable fuels is essential to accomplish this target. These renewable energy carriers have enormous unexploited energy

capital, which can satiate world energy demands at a lower price than conventional fossil fuels.

Because of its environmental advantages, biomass has gained much recognition among all renewable energy resources. Biomass refers to dry plant matter, which is abundantly available (220 billion tons annually) worldwide and is considered a low-cost renewable energy resource (Kumar et al., 2015). Waste biomass and dedicated biomass are recognized as feasible and attractive sources to produce fuel and energy. Agriculture crop residue, aquatic plants, forestry waste, and other energy crops are the major lignocellulosic biomass resources (Kumar et al., 2022), which require much processing and occupy large tracts for disposal. Consequently, repurposing the waste (by-products) into fuel and energy production reduces waste disposal issues and boosts economic profits by complete chain utilization (Ghosh et al., 2016). In addition, it is appropriate for the development of bio-based economics, which translates into the effective exploitation of biomass for fuel and power production and the ensuing employment benefits (Ghosh et al., 2016).

Biochemical and thermochemical techniques are the two consequential processes employed to transform biomass into renewable fuel and valued chemicals. The biochemical process is time-consuming, while the thermochemical process fragments the biomass within seconds or in a few minutes (depending on the applied process). Combustion, gasification, pyrolysis, and hydrothermal liquefaction are the recognized thermochemical conversion processes. Among them, pyrolysis has gained more attraction due to its wide applications. Pyrolysis is the process of thermal cracking that fragments organic substances in a restricted supply of oxygen at moderate temperatures (400-700 °C). Among all the thermochemical conversions, only pyrolysis has the ability to transform materials into three diverse forms of energy (solid, liquid, and gas). Overall, biomass pyrolysis into liquid fuel and biochar is a more effective conversion technology than other thermochemical processes (Liu et al., 2015). Further, material decomposition through pyrolysis occurs with lower power consumption and a higher conversion rate.

Native to the Indian subcontinent, the Sal wood tree (*Shorea robusta*) is a perennial tree in the family *Dipterocarpaceae*. Its geographical coverage extends south of the Himalayas, including Myanmar, Nepal, India, and Bangladesh. In India, it stretches over the eastern states of Assam, Bengal, Odisha, and Jharkhand (Ashton, 2011). Sal tree may grow to heights of 30-35 m and has a trunk diameter of up to 2-2.5 m. Its leaves are 10-25 cm long and 5-15 cm wide (Ashton, 2011). With firm, coarse-grained wood that is pale in color when freshly cut but turns dark brown with exposure,

Sal wood is one of the most significant sources of hardwood timber in India and the subcontinent.

The study of the physicochemical characterization of *S. robusta* and its thermal pyrolysis revealed the potential of its biomass to produce liquid fuel and biochar (Siddiqi et al., 2020). The physicochemical features of fuel made from Sal wood sawdust (SW) showed its high potential as a fossil fuel substitute (Hasan et al., 2020). While thermal pyrolysis of Sal seeds into a liquid product revealed that the properties of liquid products needed to be upgraded before use as a transportation fuel (Singh et al., 2014). The thermal pyrolysis of biomass into a liquid fuel product has some drawbacks, such as the product's high viscosity, oxygen content, acidity, and moisture content, necessitating enhancing the properties of liquid oil using catalysts.

Catalytic pyrolysis boosts the reaction rate, enhances the yield, and results in enhanced properties of products. Also, the effective use of catalysts boosts the transformation efficiency, reduces the rate of tars generation, and increases the targeted product yield (Mishra and Mohanty, 2019). Different types of catalysts, such as calcium oxide (CaO), copper oxide (CuO), and aluminum oxide (Al<sub>2</sub>O<sub>3</sub>), have been applied to boost the yield and characteristics of products. In a study, it was verified that using CaO improved the hydrogen percentage by decreasing the carbon dioxide, while as a reactant, CaO increased the ketones in the pyrolytic oil by reducing the acids (Wang et al., 2020). CaO also increased the furans and hydrocarbons by decreasing the ester and anhydrosugar content. It has also been experimentally shown that introducing copper oxide (CuO) yielded uniform product distribution during pyrolysis. In addition, it improved tar yield, reduced the polycyclic aromatics hydrocarbons (PAH), and increased the relative content of phenols (Mishra and Mohanty, 2019). The high-oxygen-containing acids may be eliminated during biomass pyrolysis in the presence of CaO, while more hydrocarbons can be formed in bio-oil (Chen et al., 2021). The introduction of Al<sub>2</sub>O<sub>3</sub> during pyrolysis substantially increased the light fraction products and reduced the amount of brominated products (Ozbay et al., 2018). Chen et al. (2017) investigated the various roles of CaO over cotton stalk in a fixed bed reactor and reported that using CaO increased the furans and hydrocarbons by decreasing the ester and anhydrosugar (Chen et al., 2017). Cheng and Wu (2017) also studied the effect of varying percentages of CuO (1, 3, 5, 10, and 15%) on the moso-bamboo in a tubular reactor and found that adding 5 wt% of CuO increased the yield of phenol in bio-oil and decreased the polycyclic aromatic hydrocarbons. Mishra and Mohanty (2019) studied the pyrolysis of pine sawdust and Gulmohar seeds to produce fuel and chemicals in a semi-batch reactor. They suggested that using the catalysts improved the fuel properties and yielded at optimized conditions. Chen et al. (2021) revealed that CaO catalyst produced from calcium d-gluconate monohydrate showed superior deoxygenation performance compared to CaO obtained from Ca(OH)<sub>2</sub>, with hydrocarbon yields reaching up to 27 wt%.

In light of the studies mentioned above gaps, to the best of the authors' knowledge, limited research has been conducted on the use of low-cost catalysts (i.e., CaO, CuO, and Al<sub>2</sub>O<sub>3</sub>) in the pyrolysis of SW. While the production and characterization of biochar from SW seem entirely missing. Therefore, the current study investigated the effects of different low-cost catalysts on the pyrolysis process of SW. Using low-cost catalysts such as CaO, CuO, and Al<sub>2</sub>O<sub>3</sub> with three loading rates (10, 20, and 30 wt%), the pyrolysis test was carried out in a cylindrical-shaped semi-batch reactor. Additionally, optimization efforts were made to address process limitations such as temperature, heating rate, and biomass to catalyst loading (B/C). Furthermore, pyrolytic oil was characterized by employing Fourier-transform infrared spectroscopy (FTIR), gas chromatograph-mass spectrometry (GC-MS), and elemental analyzers (C, H, N, and S), whereas biochar was analyzed using proximate analysis, elemental analysis, Brunauer-Emmett-Teller (BET) surface analysis, field emission scanning electron microscopy (FESEM), thermogravimetric analysis (TGA), and FTIR.

## 2. Materials and Methods

### 2.1. Sample collection and preparation

SW was collected from the wood mills located in Guwahati, Assam, India. The collected feedstock was sundried for one week and then stored in a sealed glass jar to evade humidity absorption. After that, the preserved biomass was milled into the targeted particle size (800-850 μm) by a home mixture grinder. The ground biomass was again stored in the airless glass jar. The biomass

sample was dried overnight in a hot air oven at 60 °C for uniform elimination of humidity before each experiment.

### 2.2. Characterization of fresh and calcined catalysts

Before the experiment, all the catalysts (CaO, CuO, and Al<sub>2</sub>O<sub>3</sub>) were calcined in a muffle furnace at 900 °C for 6 h. The catalysts were purchased from Thermo Fisher Scientific India Private Limited. Additionally, using the BET, X-ray diffraction (XRD), and FESEM, CaO, CuO, and Al<sub>2</sub>O<sub>3</sub> were studied before and after calcination. Under a nitrogen environment, the surface area of un-calcined and calcined catalysts was measured using a BET surface area analyzer (Tristar II; Micromeritics, USA) surface area analyzer. Before nitrogen adsorption, the sample was degasified for 5 h in a vacuum at 300 °C. Furthermore, an XRD diffractometer (D8 Advance, Bruker, Netherlands) was used to measure the change in crystallinity. CuK radiation was used to perform the scanning from 5-90° at a scanning step of 0.02. Using FESEM (Zeiss, Sigma 300), catalysts' surface morphology and microstructure alteration were studied.

### 2.3. Physicochemical study

The proximate examination was carried out following ASTM D 3173-3187 and D 3175-89. Perkin-Elmer elemental analyzer (Thermo scientific Flash 2000) was used for the elemental results. An oxygen bomb calorimeter (Model 1341 Plain Jacket Calorimeter, Parr Instrument) was used to estimate the sample's higher heating value (HHV). In addition, TGA was used to study the feedstock's composition (hemicellulose, cellulose, and lignin).

### 2.4. Thermal stability analysis

The thermal stability of the sample was analyzed using TGA (STA-7200, Hitachi) by providing the decomposition temperature regime of the sample in a non-oxidative environment. Briefly, about 8.0±0.12 mg of powder feedstock was positioned in the pan and heated from 25-900 °C at a heating rate of 10 °C/min with a steady nitrogen flow rate (50 mL/min).

### 2.5 FTIR analysis

FTIR analysis of SW and Sal wood sawdust biochar (SWC) was investigated using a Shimadzu FTIR analyzer (IRAffinity-1; Shimadzu, Japan). A thin layer of a liquid or powdered sample free of moisture was applied to the attenuated total reflectance (ATR) crystal. The scanning was carried out in the 400-4000 cm<sup>-1</sup> wavelength range at a rate of 40 and a step size of 4 cm<sup>-1</sup>.

### 2.6. Process parameter optimization

Process limitations (temperature, rate of heating, size of the particle, reactors types, types of biomass and its chemical constituents, etc.) significantly impact the yield and characteristics of the final pyrolysis products. The two factors that influence a process most are temperature and heating rate. To get the maximum liquid yield, five temperatures (400, 450, 500, 550, and 600 °C) and three heating rates (50, 80, and 100 °C/min) were proposed in this study. The effects of adding catalysts on the yield of pyrolytic products and their characteristics were also optimized. The uniform mixture of biomass and catalysts were filled in the reactor manually. Three ratios (10, 20, and 30 wt%) were proposed to optimize the catalyst loading. Throughout the test, the sweeping gas flow remained constant (100 mL/min). The experiment was conducted in triplicate, and average data were reported.

### 2.7. Pyrolysis setup and experiments

A stainless steel cylindrical (semi-batch reactor, SS-304) with dimensions of 4 cm ID, 4.6 cm OD, and 30 cm in length was used for the pyrolysis experiment. The main parts of the experimental setup were the control panel, thermocouple, condenser, water chiller, nitrogen gas cylinder, and rotameter. Dry biomass (50 g) was fed inside the reactor,

which was then positioned vertically inside the ceramic furnace. The furnace was constructed to ensure even heating throughout the reactor uniformly. The temperature, residence time, and heating rate were all regulated by a PID controller mounted with a control panel. To remove unwanted impurities from the reactor, the nitrogen gas was allowed to flow for 15 min before the tests. The nitrogen gas flow rate was controlled by a rotameter during the pyrolysis process. The condenser was attached to the top end of the reactor, while the nitrogen gas input was located at the bottom end. Throughout the trials, a water chiller was used to continuously circulate the cold water (8-10 °C) inside the condenser while the non-condensable gases were left outside the collecting tank. The condensable gases were condensed in the condenser and collected in a conical flask. **Figure 1** depicts the complete laboratory experimental setup used in the present study. Finally, the reactor was cooled to room temperature before collecting the biochar, and the liquid yield, char yield, and syngas, whose yields were calculated using **Equations 1-3**.

$$\text{Liquid yield (\%)} = [\text{weight of liquid fuel}/\text{weight of total feed}] \times 100 \quad \text{Eq. 1}$$

$$\text{Char yield (\%)} = [\text{weight of remaining char}/\text{weight of total feed}] \times 100 \quad \text{Eq. 2}$$

$$\text{Gas yield (\%)} = 100 - (\text{liquid yield} + \text{char yield}) \quad \text{Eq. 3}$$

### 2.8. Characterization of pyrolytic oil

The pyrolytic liquid was left overnight in the separating funnel to allow the separation of the organic and aqueous phases by density difference: the top layer as organic oil or pyrolytic oil and the bottom layer as the aqueous phase. The viscosity of pyrolytic oil was assessed using HAKKE Rheostress 1, Cone (Meas. Cup Z 43 (Series 1)), and Plate (PP 35 Ti, D=35 mm) type geometry at 40 °C at 50 RPM. The moisture content of pyrolytic oil was determined using a Karl Fischer water analyzer (Metrohm 787 KF Titrimo), whereas a Eutech waterproof (pH Spear) pH meter was also used to measure the acidity. A density meter (Anton Paar) was used to measure the density. Average results were recorded after injecting 1 mL of organic oil free of air into the density meter. An oxygen bomb calorimeter (1341 Plain Jacket Calorimeter) was used to measure the HHV of the fuel. The DIN EN-7 standard was also used to assess the pyrolytic oil ash content. A hot air oven operating at 105 °C for 1 h was used to eliminate the moisture content of pyrolytic oil. One g of dried pyrolytic oil was placed in a ceramic crucible that had been dried and weighed, and it

was heated for 24 h at 775 °C. The sample was removed from the muffle furnace once the experiment was finished and placed in a desiccator for isothermal cooling. The amount of ash in pyrolytic oil was determined by the difference between the initial and final weights.

### 2.9. GC-MS analysis

A gas chromatograph-mass spectrometer (Varian, 450-GC, 240-MS; Netherlands) was used to analyze pyrolytic oil to identify the organic fraction. Elite 5 MS column (diameter 0.250 mm, length 30 m) allowed the identification of the hot vapor. Throughout the study, helium (purity of 99.99%) was used as carrier gas with a flow rate of 1 mL/min. Additionally, 1 µL of the sample was added after 100:1 (vol/vol) of dichloromethane was employed as a dilution solvent with pyrolytic oil. GC was configured to start at 40 °C for 1 min, ramp up to 280 °C at 5 °C/min, and then hold for 15 min to allow for the extraction of all constituents. Injector, interface, and MS ion source temperatures were maintained at 280 and 250 °C, respectively. While the electron ionization voltage remained at 70 eV, the injector split ratio remained constant at 10:1. By comparing the acquired mass spectra with the database of the National Institute of Standards and Technology (NIST), it was possible to identify the unidentified products in the organic oil. All the analyses were performed in triplicate.

### 2.10. Characterization of biochar

This study examined the characteristics of biochar produced by thermal pyrolysis at 500 °C, 80 °C/min heating rate, and 100 mL/min gas flow rate. The proximate analysis of SWC was conducted based on the ASTM D 3173-3187 and ASTM D 3175-89 standards. Additionally, an elemental analyzer was used to conduct the elemental analysis of SWC. The HHV of biochar was measured using an oxygen bomb calorimeter (Model 1341 Plain Jacket Calorimeter, Parr Instrument). Additionally, a graduated cylinder and digital balance were used to calculate the bulk density of SWC. FESEM (Zeiss, Sigma 300) was used to investigate the surface morphology, whereas a BET surface area analyzer (Tristar II; Micromeritics, U.S.A.) was used to measure the BET surface area of SWC. The biochar was vacuum-degasified for 4 h at 200 °C before N<sub>2</sub> adsorption. Further, using a particle size analyzer (Delsa Nano C, Beckman Coulter,

**Fig. 1.** Laboratory-scale experimental pyrolysis setup.

Nyon, Switzerland), the zeta potential of SWC was determined. A flow rate of 1 cm<sup>3</sup> of the centrifuged SWC and water mixture was introduced into the analyzer. A pH meter (Orion 720A Model) was used to measure the pH following ASTM D4972. Further, using a portable thermal conductivity meter, the electrical conductivity (EC), thermal conductivity (TC), thermal diffusivity (TD), and specific heat of SWC were measured.

### 3. Results and Discussion

#### 3.1. Characterization of catalysts

XRD diffraction spectra of raw and calcined catalysts (CaO, CuO, and Al<sub>2</sub>O<sub>3</sub>) are shown in Figures 2a, b, and c, respectively. The diffraction peaks obtained at 17.85, 28.74, 46.90, 54.18, and 62.65° agree with the standard of the Joint Committee on Powder Diffraction Standards file (JCPDS-82-1691) for CaO (Balázs et al., 2007). XRD diffraction results indicated that the catalysts had a semi-crystalline structure. The peak obtained at 32.63, 35.34, 38.88, 48.92, 61.47, 66.09, and 67.99° for CuO and 14.44, 28.25, 34.79, 38.24, 42.44, 49.35, and 67.43° for Al<sub>2</sub>O<sub>3</sub> are in good alignment with the JCPD (Fernandes et al., 2009). Results showed that the calcined catalysts, such as CaO and CuO, did not show changed phases but altered peak intensity (sharp peaks) due to molecular adhesion triggered by the higher temperature. When molecules adhere to each other, that leads to an increase in crystal size, allowing the formation of sharp peaks. However, in the case of Al<sub>2</sub>O<sub>3</sub>, phase change was due to calcination, thus, yielding sharp peaks. The surface areas of the applied catalysts analyzed using BET are tabulated in Table 1. It was found that the BET surface area of calcined CaO, CuO, and Al<sub>2</sub>O<sub>3</sub> was decreased (1.52, 3.66, and 48.04 m<sup>2</sup>/g) due to the formation of bigger crystalline forms than raw catalysts (3.66, 8.30 and 153.04 m<sup>2</sup>/g for CaO, CuO, and Al<sub>2</sub>O<sub>3</sub> respectively). The pore diameter of the raw catalysts is higher than the calcined catalysts due to adhering of molecules, altering the pore structure and their diameter (Fig. 3). Similar patterns were also observed in the FESEM image of the applied catalysts. The FESEM images presented in Figures 3a-f demonstrate a distinct change in texture (such as the shape of the surface or substance) and structure (such as the cohesive whole built up of distinct parts) of catalysts due to thermal treatment.

**Table 1.**  
BET surface area analysis of the catalysts used before and after calcination.

Catalyst	BET surface area (m <sup>2</sup> /g)	Pore diameter (nm)
CaO	3.66±0.012	16.09±0.001
CaO-900	1.52±0.015	4.37±0.002
CuO	8.30 ±0.12	16.09±0.004
CuO-900	3.66±0.011	4.38±0.002
Al <sub>2</sub> O <sub>3</sub>	153.04±0.42	20.97 ±0.001
Al <sub>2</sub> O <sub>3</sub> -900	48.04±0.12	6.77±0.002

#### 3.2. Physicochemical characterization

The physicochemical results of SW compared to other biomass types are listed in Table 2, including cotton stalk (Raj et al., 2015), sugarcane bagasse (Raj et al., 2015), *Cynodon dactylon* (Mishra et al., 2020b), and corn cobs (Raj et al., 2015). The proximate analysis study of SW established 76.03% volatile matter, 6.04% moisture content, 2.02% ash content, and 15.99% fixed carbon. The higher volatile matter and lower ash content of SW compared to the other biomass types listed in Table 2 could be regarded as an indication of the higher ignition efficiency of this biomass (Mishra et al., 2020b). Ash content has an inverse correlation with heating value (Mishra et al., 2020b), while high ash contents could also cause fouling and slagging issues in the boilers (Doshi et al., 2014), mostly because of ash deposition. The moisture content of SW was measured at 6.04% which was less than the permitted limits (10%) (Mishra and Mohanty, 2018a). The ultimate analysis of SW showed 50.43% carbon, 5.99% hydrogen, 43.06% oxygen, and 0.52% nitrogen, while no sulfur content was detected. Hence, given SW's low nitrogen content and zero sulfur, it could be

**Fig. 2.** XRD analysis of raw and calcined catalysts used in this study (a) CaO, (b) CuO, and (c) Al<sub>2</sub>O<sub>3</sub>.

deduced that its pyrolysis would result in low SO<sub>x</sub> and NO<sub>x</sub> emissions (Mishra and Mohanty, 2018a). SW's extractives content stood at 11.23%,

**Fig. 3.** Field emission scanning electron microscopy (FESEM) analysis of the catalysts used in this study (a) CaO, (b) calcined CaO, (c) CuO, (d) calcined CuO, (e) Al<sub>2</sub>O<sub>3</sub>, and (f) calcined Al<sub>2</sub>O<sub>3</sub>.

**Table 2.**  
Physicochemical characteristics of Sal wood sawdust compared to other biomass types.

Analysis	Sal Wood Sawdust	Cotton Stalk <sup>a</sup>	Sugarcane Bagasse <sup>a</sup>	<i>Cynodon Dactylon</i> <sup>b</sup>	Corn Cob <sup>a</sup>
<i>Proximate analysis (wt%)</i>					
Moisture content	6.04±0.2	8.9	10.0	3.2.0±0.6	10.2
Volatile matter	76.03±0.1	71.0	76.0	70.89±0.84	80.0
Ash content	2.02±0.01	3.5	4.4	11.34±0.18	5.7
Fixed carbon	15.99±0.2	16.6	9.6	14.57±0.17	4.2
<i>Ultimate analysis (wt%)</i>					
C <sup>1</sup>	50.43	46.8	43.2	44.86±0.2	44.2
H	5.99	6.4	6.2	5.57±0.1	5.9
O	43.06	46.8	43.2	47.64±0.2	44.2
N	0.52	0.3	0.4	1.23±0.1	0.54
S	-	0.2	0.8	0.70±0.1	0.08
Heating value (MJ/kg)	19.18 ± 09	19.2	17.2	17.96±1.6	15.5
Bulk density (kg/m <sup>3</sup> )	330.12± 20	-	-	456.0±1.8	-
Chemical analysis (wt%)	78.95	81.10	75.1	81.00	77.0
Hemicellulose (HC)	16.23	19.2	18.7	18.98±0.24	29.0
Cellulose (C)	49.52	39.4	36.6	43.56±0.26	32.2
Lignin (L <sub>g</sub> )	13.20	23.2	19.8	18.46±0.18	15.8
Extractive content (wt%)	11.23	7.6	19.4	-	14.8
Hexane/water	10.02 ±0.12	6.2	17.2	12.00±1.4	12.3
Ethanol	1.21 ±0.11	1.4	2.2	7.00±1.2	2.5

<sup>1</sup> C, H, N, O, and S denote carbon, hydrogen, nitrogen, oxygen, and sulfur, respectively.

<sup>a</sup> Raj et al. (2015)

<sup>b</sup> Mishra et al. (2020b)

like other reported biomass in Table 2. It has been established that biomass containing higher extractives content would favor more liquid fuel generation during pyrolysis (Guo et al., 2010).

### 3.3. Thermal stability analysis

The thermal stability of SW was performed using TGA in a non-oxidative ambiance. From the TGA curve (Fig. 4), it could be noticed that SW passed through three main stages: drying, devolatilization (active pyrolysis stage), and finally, biochar establishment. The initial stage is the dehydration phase, where moisture content and very light volatile matter eviction occur (up to 150 °C). The second stage (150-500 °C) is identified as devolatilization or active pyrolytic zone, where the maximum degradation happens. In the 2<sup>nd</sup> stage, higher molecular weight products split into several smaller molecular weight products, aided by the supply of continuous heat, generating hemicellulose and cellulose as the main constituents of decomposition. At the last stage, lignin decays at a gentler rate, requiring higher temperatures (>500 °C) due to its greater thermal stability associated with the hydroxyl phenolic groups of this compound (López-Beceiro et al., 2021). Considering the derivative thermogravimetric (DTG) curve (Fig. 4), the first peak (65 °C) could be attributed to the eviction of humidity and very light volatile products at around 150 °C. The 2<sup>nd</sup> peak formed due to the breakdown of hemicellulose, while the 3<sup>rd</sup> peak arose from the decomposition of cellulose. It is well established that the decomposition profile of the lignocellulosic biomass begins with hemicellulose and then shifts towards cellulose and lignin sequentially (Kumar et al., 2019). Further, it was observed that SW decomposed 9% in the 1<sup>st</sup> stage and 68.68% in the 2<sup>nd</sup> stage. Lignin decomposed at higher temperatures due to its structure and contained functional groups. Lignin is made of cross-linked mononuclear polymers of higher carbon content connected with an asymmetrical structure of hydroxyl along with methoxy-substituted phenylpropane elements. It was also reported that the char generation at the

time of pyrolysis would depend on the lignin content; thus, the lignin content of biomass is directly proportional to char formation (Shahbaz et al., 2022).

### 3.4. Effect of temperature and heating rate on pyrolysis products yield

The process parameters of pyrolysis include temperature and heating rate, which are the main variables directly affecting the yield and characteristics of the products. This work examined the effects of temperature and heating rate on the pyrolysis of SW, and the findings are displayed in Figure 5. The greatest yield of pyrolytic oil (46.02 wt%) was measured at 500 °C due to complete biomass pyrolysis. The biomass particles were entirely pyrolyzed due to increased heat and mass exchange, encouraging the maximum discharge of hot volatiles. The production of pyrolytic liquid was lower (38.66 and 43.25 wt%), and the biochar yield was higher (34.25 and 28.56 wt%) at lower temperatures, like 400 and 450 °C, respectively, which could be ascribed to less contact between the biomass particles. In other words, lower temperatures result in fractional pyrolysis, producing more biochar and less pyrolytic liquid. It was also noted that the CO<sub>2</sub> generation was higher at lower temperatures which was in line with the results reported by previous studies (Kongkasawan et al., 2016), while the yield of hydrogen gas was lower.

Additionally, according to data presented in Figure 5, the quick endothermic breakdown of biomass at higher temperatures (550 and 600 °C) resulted in a decrease in liquid and char yield and an increase in gas yield. Equations 4 and 5 suggest an endothermic reaction at higher temperatures (>500 °C), leading to the secondary cracking and reforming reactions reducing the yield of pyrolytic liquid while considerably increasing the generation of non-condensable gases, likely H<sub>2</sub> and CO (Zhang et al., 2007; Zaman et al., 2017). The dehydration reaction is also responsible for the generation of the aqueous phase. More specifically,

**Fig. 4.** Thermal stability profile of Sal wood sawdust (SW) at 10 °C min<sup>-1</sup> heating rate (a) TGA and (b) DTG.

**Fig. 5.** Effect of (a) temperature and (b) heating rate on the yield of the pyrolysis products.

during catalytic pyrolysis, O<sub>2</sub> reacts with H<sub>2</sub> and produces H<sub>2</sub>O, leading to a decline in the viscosity and oxygen content of the pyrolytic oil (Mishra and Mohanty, 2018b).

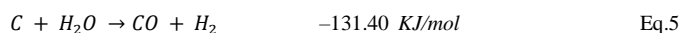
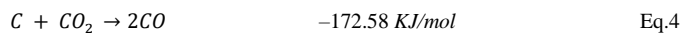


Figure 5 also depicts the impact of heating rates on the pyrolysis of SW. As presented, the largest liquid production (46.02 wt%) was recorded at

80 °C/min heating rate caused by complete biomass pyrolysis. Partial pyrolysis of the feedstock at the lower heating rate (50 °C/min) reduced the liquid production by 2-3%. On the other hand, due to the rapid endothermic degradation of the feedstock at the increased heating rate of 100 °C/min, which turned condensable gases into syngas, the yield of liquid also declined (Uddin et al., 2013). It has been determined that a higher heating rate is preferable for obtaining accurate product compositions; however, system efficiency must be considered (Debdoubi et al., 2006). Hence, the optimal pyrolysis conditions were found to be 500 °C and an 80 °C/min heating rate; nevertheless, the flow rate of sweeping gas remained constant (100 mL/min) throughout the test.



### 3.5. Effect of catalysts on pyrolytic products yields

The impact of catalyst loading on the yield of pyrolysis products is presented in **Figure 6**, where it can be noticed that the catalyst loading of 20 wt% produced the maximum liquid yield (compared to 10 and 30 wt%).

It is essential to mention that the catalyst loading 5 wt% was also tested, but the effect on pyrolysis yields was negligible; hence, it is not reported herein. However, at 20 wt% of catalyst loading, the liquid yield was increased (50.02 and 48.23 wt%) for CaO and CuO, respectively, whereas in the case of Al<sub>2</sub>O<sub>3</sub>, the liquid yield decreased (43.23 wt%). Such analogous outcomes were also reported for the pyrolysis of *Pinus ponderosa* and *Delonix regia* biomass previously (Mishra and Mohanty, 2019). Positive synergistic effects between the biomass and catalyst particles lower the reaction's activation energy and could be regarded as the reason leading to increased pyrolytic liquid yield at optimal catalyst loading rates.

### 3.6. Characterization of pyrolytic oil

The physicochemical characteristics of the pyrolytic oil produced through thermal and catalytic pyrolysis using different catalysts are presented in Table 3 and compared with those of diesel fuel. Both thermal and catalytic pyrolytic oil had a smoky smell and dark brown color. The elemental composition of the pyrolytic oil revealed that the functionalized catalysts substantially increased the carbon content (74.28, 17.60, and 70.62%) and reduced the oxygen content (16.60, 19.07, and 19.66%) for CaO, CuO, and Al<sub>2</sub>O<sub>3</sub> respectively. The higher content of oxygenated products in pyrolytic oil may alter the stability, flame temperature, and fluidity (Mishra et al., 2020a). All pyrolytic oils contained less nitrogen; hence, it could be concluded that less nitrogen oxide would be generated during their combustion in engines compared to diesel fuel (Table 3). Another important factor in choosing the right fuel is its viscosity (Yuan et al., 2018). The pyrolytic oil's viscosity was dramatically dropped once catalysts were used, making it more appropriate for engine use than the thermal pyrolytic oil. However, the viscosity of all three catalytic pyrolytic oils obtained was still much larger than that of diesel fuel, necessitating their blending with diesel to achieve a proper engine performance.

Due to the decreases in O<sub>2</sub> content, which raised the hydrogen-to-carbon ratio of the oil, the HHV of catalytic pyrolytic oil was found to be 36.09, 34.92, and 33.29 MJ/kg for CaO, CuO, and Al<sub>2</sub>O<sub>3</sub>, respectively, which were considerably higher than that of thermal pyrolytic oil (25.66 MJ/kg). The higher the HHV of pyrolytic oil, the larger the energy content of the fuel and a more suitable alternative for diesel to be used in the transportation sector. As for the moisture content, the hydration process must have elevated the catalytic pyrolytic oil's moisture over that of thermal pyrolytic oil (Mishra et al., 2020c). The moisture content of the pyrolytic oil could result in increased atomization and improved combustion in diesel engines (Panchasara and Ashwath, 2021). The acidity analysis exhibited a lower acidity for catalytic pyrolytic oil (9.6, 8.4, and 7.5 for CaO, CuO, and Al<sub>2</sub>O<sub>3</sub>, respectively) vs. thermal pyrolytic oil (4.2). The higher fuel acidity has a detrimental effect on its heating value due to the presence of proton ions forming water molecules by reacting with oxygen (Mishra et al., 2020c). The bulk density of the thermal pyrolytic oil was lower (907 kg/m) than catalytic pyrolytic oil (911, 914, and 913 kg/m for CaO, CuO, and Al<sub>2</sub>O<sub>3</sub>, respectively). Finally, the ash content analysis suggested that catalytic pyrolytic oils had lower ash contents (0.12, 0.11, and 0.16% for CaO, CuO, and Al<sub>2</sub>O<sub>3</sub>, respectively) than thermal pyrolytic oil (0.26%), rendering them more suitable for use as a transportation fuel. Also, the use of catalysts limited tars formation, which must have contributed to reducing the ash content.

### 3.7. FTIR analysis of pyrolytic oil

The presence of favorable functional groups in the pyrolytic oil was found using the FTIR analysis (Fig. 7). Water, phenols, and aromatics were detected based on the adsorption band observed between 3500 and 3300 cm<sup>-1</sup>, attributable to -OH stretching vibration (Cardona-Urbe et al., 2021). The occurrence of alkane was indicated by the adsorption band between 2960 and 2850 cm<sup>-1</sup>, caused by C-H stretching vibration (Mishra et al., 2019). The peak at 1714 cm<sup>-1</sup> demonstrated the presence of ketone groups because of C=O stretching vibrations. The presence of aromatics and alkene was reflected at the peak of 1620 cm<sup>-1</sup> due to C=C stretching vibrations (Mishra et al., 2022c). The peak at 1330-950 cm<sup>-1</sup> associated with the C-O stretching revealed the presence of ester and ethers and the deformation of these functional groups, whereas the peak at 1453 cm<sup>-1</sup> arose from the C-C

**Fig. 6.** Effect of catalyst loading on the yield of catalytic pyrolytic products of SW at optimized conditions (a) CaO, (b) CuO, and (c) Al<sub>2</sub>O<sub>3</sub>.

**Table 3.**  
Physicochemical characteristics of Sal wood sawdust compared to other biomass types.

Analysis	Thermal	CaO	CuO	Al <sub>2</sub> O <sub>3</sub>	Diesel
Colour	Dark brown	Dark brown	Dark brown	Dark brown	Orange
Odor	Smoky	Smoky	Smoky	Smoky	-
Carbon (%)	61.79±0.2	74.28±0.21	71.6±0.19	70.62±0.2	86.60
Hydrogen (%)	6.29±0.11	7.02±0.1	7.43±0.1	7.32±0.1	13.28
Oxygen (%)*	28.32±0.23	16.6±0.26	19.07±0.2	19.66±0.24	0.01
Nitrogen (%)	2.63±0.1	2.12±0.14	2.53±0.16	2.46±0.12	6.51
Sulfur (%)	0.89±0.06	0.35±0.09	0.65±0.08	0.35±0.04	0.10
HHV (MJ/kg)	25.66±0.2	36.09±0.2	34.92±0.4	33.29±0.6	45.50±0.2
Viscosity (cSt) at 40 °C	69.5±1.8	22±1.3	24.6±1.6	23.56±1.4	2-4.5
Acidity (pH)	4.2±0.8	9.6±0.6	8.4±0.8	7.5±0.4	-
Moisture (%)	1.2±1.3	1.86±1.3	1.91±1.2	1.84±1.5	-
Density (kg/m <sup>3</sup> )	907±2.1	911±2.4	914±1.8	913±1.6	810-828
Ash content (wt%)	0.26±0.12	0.12±0.11	0.11±0.12	0.16±0.14	-

\*Oxygen was calculated by difference.

**Fig. 7.** FTIR spectra of thermal and catalytic pyrolytic oil.

bond representing the alkyne groups (Garg et al., 2016). Additionally, the mono- and polycyclic substituted aromatic compounds could be attributed to the peak at 900-500 cm<sup>-1</sup> caused by O-H bending (Mishra et al., 2022b).

### 3.8. GC-MS analysis of pyrolytic oil

The chromatographs obtained from the GC-MS were compared to the NIST library and the published literature, and the pictorial representation of the main products is shown in Figure 8. Pyrolytic oil is ideal for engine application due to its high content of hydrocarbons, aromatics, acids, esters, phenols, furan derivatives, alkanes, ketones, ethers, and aldehydes (Chen et al., 2015; Mishra et al., 2020a). More intriguingly, the chemical constituents of the biomass used to make pyrolytic oil could change its composition, making it difficult to forecast the exact makeup of the oil. Acids, ketones, cycloalkane, furanic products, and mixed hydrocarbons are the main results of the breakdown of hemicellulose and cellulose (Lu et al., 2010; Ma et al., 2020), while the decomposition of lignin yields mostly guaiacyl, p-hydroxyphenyl, syringyl, aromatic hydrocarbons, and various other hydrocarbons (Hidayat et al., 2018). According to the GC-MS data, the thermal pyrolytic oil obtained herein contained 12.3% hydrocarbons, 20.23% phenols, 12.23% acids, 4.21% ketone, 8.26% ether, 2.1% furan derivatives, 5.56 % alcohol, 2.5% esters, 6.62% nitrogen-containing compounds, 5.2% aldehyde, and 3.3% amide groups.

**Fig. 8.** Compositional analysis of pyrolytic oil using GC-MS analyzer.

Similar results were also reported for the pyrolysis of pine wood and waste plastics (waste nitrile gloves (WNG) and polystyrene (PS)) (Mishra et al., 2022a) and groundnut shells (Kumar et al., 2021). When the primary goal is the application of pyrolytic oil as a transportation fuel, acids would be considered unfavorable, adversely affecting the fuel properties (Mohan et al., 2006). Compared to the thermal pyrolytic oil, the concentration of the acidic products in the catalytic pyrolytic oils decreased substantially by 7.25, 6.56, and 9.25% for CaO, CuO, and Al<sub>2</sub>O<sub>3</sub>, respectively, due to the transformation of acids into ketones and alcohols. A similar result was reported for the pyrolysis of *Nannochloropsis oculata* (Gautam and Vinu, 2018) and waste dahlia flowers (Mishra et al., 2020c). The catalytic pyrolytic oil also contained a reduced concentration of phenols, i.e., by 15.26, 16.79, and 16.52% for CaO, CuO, and Al<sub>2</sub>O<sub>3</sub>, respectively, compared to the thermal pyrolytic oil, due to the deoxygenation reactions resulting in the conversion of phenols into several aromatics hydrocarbons (Lu et al., 2018). Similar findings were obtained during the pyrolysis of waste dahlia flowers (Mishra et al., 2020c).

The introduction of catalysts significantly increased the water content of the pyrolytic oil by reacting oxygen with hydrogen molecules, reducing esters and ethers contents, and stimulating a substantial increase in aldehydes content due to the conversion of acids into aldehyde (Mishra et al., 2020c). The applied catalysts also significantly reduced the nitrogen-containing compounds by transforming the deamination reaction (Setter et

al., 2020). The addition of catalysts enhanced the ratio of furans and their derivatives, as the breakdown of hemicellulose and celluloses would mostly produce these compounds (Hidayat et al., 2018). The moisture content of biomass evaporates at the temperature of ~100 °C due to the acceleration of the dehydration reaction. This phenomenon could significantly increase amorphous carbon in the resultant biochar during the pyrolysis process (White et al., 2011). In general, the feedstock characterization (e.g., elemental and proximate analyses and type of the chemical bonds), as well as operating conditions, determines the main reaction pathway (e.g., biochar formation, depolymerization, and fragmentation) during the pyrolysis process. Biochar, a solid residue created during the biomass conversion process in pyrolysis, has an aromatic polycyclic structure. The major biochar formation route synthesizes benzene rings and their coupling with polycyclic structures. At temperatures ranging from 300 to 450 °C, biomass macromolecules (e.g., cellulose and hemicellulose) are decomposed into tiny aromatic monomers, and low molecular-weight saturated compounds. This decomposition could result in the formation of short-chain compounds and volatile matters which are condensable at atmospheric temperature (Collard and Blin, 2014). Fragmentation is the linking of covalent bonds inside monomer units, leading to the formation of non-condensable gases and linear short-chain compounds (Kan et al., 2016). The volatile matter might be introduced to secondary reactions such as cracking and repolymerization to produce higher molecular-weight constituents. These high molecular-weight compounds are not volatile under pyrolysis temperature and could be retained in liquid/solid phase products.

### 3.9. Characterization of biochar

**Table 4** presents the physicochemical characteristics of the SWC compared to some other biochars obtained from the pyrolysis of several biomass types (*Samanea saman* seeds biochar, palm shell hydrochar, ramie residue char) and coal (Nizamuddin et al., 2015; Yi et al., 2013; Mishra et al., 2020a). The higher the volatile matter and the lower the moisture content of biochar, the higher its potential for use as a dry solid fuel for domestic cooking and heating (Rafiq et

al., 2016). SWC's elemental analyses revealed that it had a significant carbon content (72.61%) and a lower nitrogen content (0.64%), making it more desirable for usage in carbon-based products (Liu et al., 2015). The HHV of SWC was measured at 30.65 MJ/kg, demonstrating the significant potential for use as a solid fuel for domestic use. SWC had a BET surface area of 5.50 m<sup>2</sup>/g, lower than those of palm shell hydrochar (12.26 m<sup>2</sup>/g) and ramie residue biochar (27.74 m<sup>2</sup>/g), limiting its effectiveness as a bio-adsorbent from the surface area perspective. However, in addition to BET surface area, Zeta potential is another co-determinant for using biochar as a bio-adsorbent, and SWC had a Zeta potential of -29.60 mV, more favorable than commercial activated carbon (-29.05 mV) (Mishra et al., 2020a).

Biochar derived from plant wastes usually yields higher acidity values caused by the presence of ash (salt or base) (Mullen et al., 2010). The results also confirmed that the obtained biochar contained salts and metals, as reflected in the SWC's pH value (7.87), possibly limiting its application in bio-adsorbents. However, using biochar with these characteristics for soil abatement or fertilizers could significantly enhance the properties of soil by releasing the base cations into the soil (Palansooriya et al., 2019). The EC of SWC was found to be 0.003812 S/m, while TC, TD, and specific heat were 0.2569 W/m.K, 0.08956 mm<sup>2</sup>/s, and 2.2987 MJ/m<sup>3</sup>.K, respectively. The EC of biochar produced from bio-oil was also in a similar range obtained in the present study (Arnold et al., 2018). The EC and TC of biochar become essential when the objective is to be introduced into energy storage devices such as fuel cells (Senthil and Lee, 2021). The oxygen/carbon (O/C) and hydrogen/carbon (H/C) molar ratios of biochar can be used to illustrate its potential as an energy source. Biochar with a higher H/C ratio could be considered a suitable energy carrier due to its high energy content. Van-Krevelen diagram can be used to show the molar ratio of the fuel. **Figure 9** presents the C/C and H/C molar ratios of SWC compared to the other types of biochars reported by previous studies using VKD. As shown, SWC has a greater H/C and a lower O/C ratio than other types of biochar, confirming its suitability for use as a coal substitute.

**Table 4.** Physicochemical characteristics of Sal wood sawdust biochar (SWC) compared with other types of biochar and coal.

Analysis	SWC*	<i>Samanea saman</i> seeds biochar <sup>a</sup>	Coal <sup>b</sup>	Palm shell hydrochar <sup>b</sup>	Ramie residue biochar <sup>c</sup>
Moisture (%)	6.45±1.1	5.14	-	-	-
Volatile matter (%)	28.33±1.5	34.14	-	-	16.91
Ash content (%)	12.25±0.68	13.18	-	-	7.54
Fixed carbon (%)	52.97±1.1	47.54	-	-	75.55
VM/FC	0.53	0.54	-	-	0.22
C (%)	70.61±0.2	62.66	55.38	63.77	79.31
H (%)	2.27±0.1	2.06	5.86	4.40	2.52
O (%)	26.38±0.2	31.83	34.07	23.33	10.45
N (%)	0.64±0.1	3.45	2.48	0.52	0.15
S (%)	-	-	2.21	1.02	0.03
O/C	0.28	0.38	-	-	0.13
H/C	1.02	0.40	-	-	0.03
Heating value (MJ/kg)	30.65±1.1	23.14	22.54	26.80	28.40
BET surface area (m <sup>2</sup> /g)	5.50	8.20	-	12.26	27.74
Bulk density (kg/m <sup>3</sup> )	257±1.2	478	-	-	-
Acidity (pH)	7.87±1.1	7.60	-	-	-
Zeta potential (mV)	-29.60±1.1	-	-	-	-
Electrical conductivity (S/m)	0.003812±2.640E-05	-	-	-	-
Thermal conductivity (W/m.K)	0.2569±0.001682	-	-	-	-
Thermal diffusivity (mm <sup>2</sup> /s)	0.08956±0.001245	-	-	-	-
Specific heat (MJ/m <sup>3</sup> .K)	2.2987±0.025689	-	-	-	-

\* C, H, N, O, and S denote carbon, hydrogen, nitrogen, oxygen, and sulfur, respectively.

<sup>a</sup> Mishra et al. (2020a)

<sup>b</sup> Nizamuddin et al. (2015)

<sup>c</sup> Yi et al. (2013)

**Fig. 9.** Van-Krevelen diagram of different types of biochar and coal char in comparison with Sal wood sawdust biochar (SWC). Data obtained from Mitchell et al. (2013), Nizamuddin et al. (2015), Yargicoglu et al. (2015), and Mishra et al. (2020a).

### 3.10. Thermal stability, FTIR, and FESEM analysis of biochar

The results of the thermal analysis of SWC using TGA are depicted in **Figure 10**. The decomposition rate of the biochar up to 800 °C was determined to be 21.82%, indicating improved thermal stability. Moisture removal was visible in the DTG peaks at 52 °C.

**Fig. 10.** Thermal analysis of Sal wood sawdust biochar (SWC) at 10 °C min<sup>-1</sup> heating rate.

However, the biochar showed the greatest disintegration at 359 and 632 °C. Using an FTIR analyzer, the biochar's functional groups were identified, and the plotted spectrum is shown in **Figure 11**. The presence of water (hydrogen-bonded hydroxyl groups) or phenolic groups was shown by the adsorption band at 3432 cm<sup>-1</sup> attributed to the -OH stretching vibration (Wang et al., 2018). The peak at 2045 cm<sup>-1</sup>, associated with the C-H stretching vibration, indicated the presence of alkanes (Wang et al., 2018; Mishra et al., 2022b). Further, the peak at 1636 cm<sup>-1</sup> could be attributed to the C=O stretching vibration representing ethers, whereas the peak at 1324 cm<sup>-1</sup> related to the C-H deformation vibrations confirmed the presence of oxygenated functional groups (Wang et al., 2018). The peak of 936 cm<sup>-1</sup> caused by the C-H out-of-plane bend represented the adjacent aromatic hydrocarbon (Wang et al., 2018). Also, the peak in the range of 500-900 cm<sup>-1</sup> exhibited polyaromatic functional groups.

**Fig. 11.** FTIR analysis of Sal wood sawdust biochar (SWC).

FESEM analysis of SWC, shown in **Figure 12**, indicated the porous structure of biochar. The results also showed that large channel-like structures proliferated the biochar surface, retaining the fractional morphology of the initial input biomass. A porous structure was created during pyrolysis by the generated hot volatiles escaping the structure.

**Fig. 12.** FESEM analysis of Sal wood sawdust biochar (SWC).

## 4. Conclusions and Prospects

The present study investigated the thermocatalytic pyrolysis of SW to produce valuable chemicals and fuels. The results from the pyrolysis in the semi-batch reactor revealed that thermal pyrolysis produced a 46.02 wt% yield of pyrolytic oil under optimized conditions while using CaO and CuO catalysts increased the yield to 50.02 and 48.23 wt%, respectively. Additionally, the attributes of catalytic pyrolytic oil were significantly improved over those of thermal pyrolytic oil, i.e., reduced viscosity, increased carbon content, lowered oxygen content, etc. The application of catalysts also lowered the oxygen-enriched products and increased the hydrocarbon content of the pyrolytic oil. It could be concluded that catalytic

pyrolytic oil could be a promising alternative for use with diesel in blended form.

The results of the biochar characterization revealed high volatile matter (28.33 wt%), heating value (30.65 MJ/kg), carbon content (72.61 wt%), zeta potential (-29.60 mV), pH (7.87), EC (0.003812 S/m), and TC (0.2569 W/m.K), rendering it suitable for a variety of industrial applications (fuel cells, supercapacitors, catalysts, bio-composite materials, etc.).

Although catalytic pyrolysis of biomass is a promising biomass valorization route, due to various variable parameters, the pyrolysis process is complex, and hence, there is a significant gap in understanding the reaction mechanisms involved. The formation of products is highly dependent on the operating conditions and types of inputs; thus, predicting a universal reaction mechanism would be difficult, possibly limiting the application of this technology on a larger scale. In light of that, considerable research is required to predict the reaction mechanisms using advanced tools such as Matlab, Density functional theory (DFT) simulation, ReaxFF, or other similar tools. Moreover, as biomass is a poor conductor of heat thus, designing suitable reactors should also be considered an essential future research need.

#### Acknowledgments

The author would like to thank the Analytic Laboratory, Department of Chemical Engineering, Indian Institute of Technology Guwahati and Department of Chemical Engineering, M.S. Ramaiah Institute of Technology Bangalore for TGA, BET, GC-MS, characterization analysis and School of Energy Science and Engineering, Indian Institute of Technology Guwahati for heating value analysis.

#### References

- [1] Arnold, S., Rodriguez-Urbe, A., Misra, M., Mohanty, A.K., 2018. Slow pyrolysis of bio-oil and studies on chemical and physical properties of the resulting new bio-carbon. *J. Clean. Prod.* 172, 2748-2758.
- [2] Ashton, P., 2011. *Shorea robusta*, IUCN.
- [3] Balázs, C., Wéber, F., Kövér, Z., Horváth, E., Németh, C., 2007. Preparation of calcium-phosphate bioceramics from natural resources. *J. Eur. Ceram. Soc.* 27(2-3), 1601-1606.
- [4] Cardona-Urbe, N., Betancur, M., Martínez, J.D., 2021. Towards the chemical upgrading of the recovered carbon black derived from pyrolysis of end-of-life tires. *Sustainable Mater. Technol.* 28, e00287.
- [5] Chen, L., Wang, X., Yang, H., Lu, Q., Li, D., Yang, Q., Chen, H., 2015. Study on pyrolysis behaviors of non-woody lignins with TG-FTIR and Py-GC/MS. *J. Anal. Appl. Pyrolysis.* 113, 499-507.
- [6] Chen, X., Chen, Y., Yang, H., Chen, W., Wang, X., Chen, H., 2017. Fast pyrolysis of cotton stalk biomass using calcium oxide. *Bioresour. Technol.* 233, 15-20.
- [7] Chen, X., Li, S., Liu, Z., Cai, N., Xia, S., Chen, W., Yang, H., Chen, Y., Wang, X., Liu, W., 2021. Negative-carbon pyrolysis of biomass (NCPB) over CaO originated from carbide slag for online upgrading of pyrolysis gas and bio-oil. *J. Anal. Appl. Pyrolysis.* 156, 105063.
- [8] Cheng, H., Wu, S., 2017. Effect of copper oxide on fast pyrolysis of enzymatic/mild Acidolysis lignin. *Energy Procedia.* 105, 1015-1021.
- [9] Collard, F.X., Blin, J., 2014. A review on pyrolysis of biomass constituents: mechanisms and composition of the products obtained from the conversion of cellulose, hemicelluloses and lignin. *Renew. Sust. Energy Rev.* 38, 594-608.
- [10] Deboudi, A., El Amarti, A., Colacio, E., Blesa, M., Hajjaj, L., 2006. The effect of heating rate on yields and compositions of oil products from esparto pyrolysis. *Int. J. Energy Res.* 30(15), 1243-1250.
- [11] Doshi, P., Srivastava, G., Pathak, G., Dikshit, M., 2014. Physicochemical and thermal characterization of nonedible oilseed residual waste as sustainable solid biofuel. *J. Waste Manage.* 34(10), 1836-1846.
- [12] Fernandes, D., Silva, R., Hechenleitner, A.W., Radovanovic, E., Melo, M.C., Pineda, E.G., 2009. Synthesis and characterization of ZnO, CuO and a mixed Zn and Cu oxide. *Mater. Chem. Phys.* 115(1), 110-115.
- [13] Garg, R., Anand, N., Kumar, D., 2016. Pyrolysis of babool seeds (*Acacia nilotica*) in a fixed bed reactor and bio-oil characterization. *Renewable Energy.* 96, 167-171.
- [14] Gautam, R., Vinu, R., 2018. Non-catalytic fast pyrolysis and catalytic fast pyrolysis of *Nannochloropsis oculata* using Co-Mo/ $\gamma$ -Al<sub>2</sub>O<sub>3</sub> catalyst for valuable chemicals. *Algal Res.* 34, 12-24.
- [15] Ghosh, P.R., Fawcett, D., Sharma, S.B., Poinern, G.E.J., 2016. Progress towards sustainable utilisation and management of food wastes in the global economy. *Int. J. Food Sci.* 2016.
- [16] Guo, X.J., Wang, S.R., Wang, K.G., Qian, L., Luo, Z.Y., 2010. Influence of extractives on mechanism of biomass pyrolysis. *J. Fuel Chem. Technol.* 38(1), 42-46.
- [17] Hasan, M.I., Mukta, N.A., Islam, M.M., Chowdhury, A.M.S., Ismail, M., 2020. Evaluation of fuel properties of Sal (*Shorea robusta*) seed and Its oil from their physico-chemical characteristics and thermal analysis. *Energy Sources Part A.* 1-12.
- [18] Hidayat, S., Bakar, M.S.A., Yang, Y., Phusunti, N., Bridgwater, A., 2018. Characterisation and Py-GC/MS analysis of *Imperata Cylindrica* as potential biomass for bio-oil production in Brunei Darussalam. *J. Anal. Appl. Pyrolysis.* 134, 510-519.
- [19] Kan, T., Strezov, V., Evans, T.J., 2016. Lignocellulosic biomass pyrolysis: a review of product properties and effects of pyrolysis parameters. *Renew. Sust. Energy Rev.* 57, 1126-1140.
- [20] Kongkasawan, J., Nam, H., Capareda, S.C., 2016. *Jatropha* waste meal as an alternative energy source via pressurized pyrolysis: a study on temperature effects. *Energy.* 113, 631-642.
- [21] Kumar, A., Kumar, N., Baredar, P., Shukla, A., 2015. A review on biomass energy resources, potential, conversion and policy in India. *Renew. Sust. Energy Rev.* 45, 530-539.
- [22] Kumar, A., Monika, Mishra, R.K., Jaglan, S., 2022. Pyrolysis of low-value waste miscanthus grass: physicochemical characterization, pyrolysis kinetics, and characterization of pyrolytic end products. *Process Saf. Environ. Prot.* 163, 68-81.
- [23] Kumar, M., Rai, D., Bhardwaj, G., Upadhyay, S., Mishra, P., 2021. Pyrolysis of peanut shell: kinetic analysis and optimization of thermal degradation process. *Ind Crops Prod.* 174, 114128.
- [24] Kumar, M., Sabbarwal, S., Mishra, P., Upadhyay, S., 2019. Thermal degradation kinetics of sugarcane leaves (*Saccharum officinarum* L) using thermo-gravimetric and differential scanning calorimetric studies. *Bioresour. Technol.* 279, 262-270.
- [25] Liu, W.J., Jiang, H., Yu, H.Q., 2015. Development of biochar-based functional materials: toward a sustainable platform carbon material. *Chem. Rev.* 115(22), 12251-12285.
- [26] López-Beceiro, J., Díaz-Díaz, A.M., Álvarez-García, A., Tarrío-Saavedra, J., Naya, S., Artiaga, R., 2021. The complexity of lignin thermal degradation in the isothermal context. *Processes.* 9(7), 1154.
- [27] Lu, Q., Guo, H.Q., Zhou, M.X., Zhang, Z.X., Cui, M.S., Zhang, Y.Y., Yang, Y.P., Zhang, L.B., 2018. Monocyclic aromatic hydrocarbons production from catalytic cracking of pine wood-derived pyrolytic vapors over Ce-Mo<sub>2</sub>N/HZSM-5 catalyst. *Sci. Total Environ.* 634, 141-149.
- [28] Lu, Q., Zhang, Z.F., Dong, C.Q., Zhu, X.F., 2010. Catalytic upgrading of biomass fast pyrolysis vapors with nano metal oxides: an analytical Py-GC/MS study. *Energies.* 3(11), 1805-1820.
- [29] Ma, C., Geng, J., Zhang, D., Ning, X., 2020. Non-catalytic and catalytic pyrolysis of *Ulva* proliferata macroalgae for production of quality bio-oil. *J. Energy Inst.* 93(1), 303-311.
- [30] Mishra, R.K., Chistie, S.M., Naik, S.U., Kumar, P., 2022a. Thermocatalytic co-pyrolysis of waste biomass and plastics: studies of physicochemical properties, kinetics behaviour, and characterization of liquid product. *J. Energy Inst.* 105, 192-202.
- [31] Mishra, R.K., Iyer, J.S., Mohanty, K., 2019. Conversion of waste biomass and waste nitrile gloves into renewable fuel. *J. Waste Manage.* 89, 397-407.
- [32] Mishra, R.K., Kumar, V., Mohanty, K., 2020a. Pyrolysis kinetics behaviour and thermal pyrolysis of *Samanea saman* seeds towards the production of renewable fuel. *J. Energy Inst.* 93(3), 1148-1162.
- [33] Mishra, R.K., Lu, Q., Mohanty, K., 2020b. Thermal behaviour, kinetics and fast pyrolysis of *Cynodon dactylon* grass using Py-GC/MS and Py-FTIR analyser. *J. Anal. Appl. Pyrolysis.* 150, 104887.
- [34] Mishra, R.K., Misra, M., Mohanty, A.K., 2022b. Value-added bio-carbon production through the slow pyrolysis of waste bio-oil:

- fundamental studies on their structure-property-processing co-relation. ACS Omega. 7(2), 1612-1627.
- [35] Mishra, R.K., Misra, M., Mohanty, A.K., 2022c. Value-added biocarbon production through slow pyrolysis of mixed bio-oil wastes: studies on their physicochemical characteristics and structure-property-processing co-relation. Biomass Convers. Biorefin. 1-15.
- [36] Mishra, R.K., Mohanty, K., 2018a. Characterization of non-edible lignocellulosic biomass in terms of their candidacy towards alternative renewable fuels. Biomass Convers. Biorefin. 8(4), 799-812.
- [37] Mishra, R.K., Mohanty, K., 2019. Thermal and catalytic pyrolysis of pine sawdust (*Pinus ponderosa*) and Gulmohar seed (*Delonix regia*) towards production of fuel and chemicals. Mater. Sci. Energy Technol. 2(2), 139-149.
- [38] Mishra, R.K., Mohanty, K., 2018b. Thermocatalytic conversion of non-edible Neem seeds towards clean fuel and chemicals. J. Anal. Appl. Pyrolysis. 134, 83-92.
- [39] Mishra, R.K., Mohanty, K., Wang, X., 2020c. Pyrolysis kinetic behavior and Py-GC-MS analysis of waste dahlia flowers into renewable fuel and value-added chemicals. Fuel. 260, 116338.
- [40] Mitchell, P.J., Dalley, T.S., Helleur, R.J., 2013. Preliminary laboratory production and characterization of biochars from lignocellulosic municipal waste. J. Anal. Appl. Pyrolysis. 99, 71-78.
- [41] Mohan, D., Pittman, C.U., Steele, P.H., 2006. Pyrolysis of wood/biomass for bio-oil: a critical review. Energy fuels. 20(3), 848-889.
- [42] Mullen, C.A., Boateng, A.A., Goldberg, N.M., Lima, I.M., Laird, D.A., Hicks, K.B., 2010. Bio-oil and bio-char production from corn cobs and stover by fast pyrolysis. Biomass Bioenergy. 34(1), 67-74.
- [43] Nizamuddin, S., Jaya Kumar, N.S., Sahu, J.N., Ganesan, P., Mubarak, N.M., Mazari, S.A., 2015. Synthesis and characterization of hydrochars produced by hydrothermal carbonization of oil palm shell. Can. J. Chem. Eng. 93(11), 1916-1921.
- [44] Ozbay, N., Yargic, A.S., Sahin, R.Z.Y., 2018. Tailoring Cu/Al<sub>2</sub>O<sub>3</sub> catalysts for the catalytic pyrolysis of tomato waste. J. Energy Inst. 91(3), 424-433.
- [45] Palansooriya, K.N., Ok, Y.S., Awad, Y.M., Lee, S.S., Sung, J.K., Koutsospyros, A., Moon, D.H., 2019. Impacts of biochar application on upland agriculture: a review. J. Environ. Manage. 234, 52-64.
- [46] Panchasara, H., Ashwath, N., 2021. Effects of pyrolysis bio-oils on fuel atomisation-a review. Energies. 14(4), 794.
- [47] Rafiq, M.K., Bachmann, R.T., Rafiq, M.T., Shang, Z., Joseph, S., Long, R., 2016. Influence of pyrolysis temperature on physico-chemical properties of corn stover (*Zea mays* L.) biochar and feasibility for carbon capture and energy balance. PloS one. 11(6), p.e0156894.
- [48] Raj, T., Kapoor, M., Gaur, R., Christopher, J., Lamba, B., Tuli, D.K., Kumar, R., 2015. Physical and chemical characterization of various Indian agriculture residues for biofuels production. Energy Fuels. 29(5), 3111-3118.
- [49] Senthil, C., Lee, C.W., 2021. Biomass-derived biochar materials as sustainable energy sources for electrochemical energy storage devices. Renew. Sust. Energy Rev. 137, 110464.
- [50] Setter, C., Silva, F.T.M., Assis, M.R., Ataíde, C.H., Trugilho, P.F., Oliveira, T.J.P., 2020. Slow pyrolysis of coffee husk briquettes: characterization of the solid and liquid fractions. Fuel. 261, 116420.
- [51] Shahbaz, M., AlNouss, A., Parthasarathy, P., Abdelaal, A.H., Mackey, H., McKay, G., Al-Ansari, T., 2022. Investigation of biomass components on the slow pyrolysis products yield using Aspen Plus for techno-economic analysis. Biomass Convers. Biorefin. 12(3), 669-681.
- [52] Siddiqi, H., Bal, M., Kumari, U., Meikap, B.C., 2020. In-depth physicochemical characterization and detailed thermo-kinetic study of biomass wastes to analyze its energy potential. Renewable Energy. 148, 756-771.
- [53] Singh, V.K., Soni, A.B., Kumar, S., Singh, R.K., 2014. Pyrolysis of sal seed to liquid product. Bioresour. Technol. 151, 432-435.
- [54] Uddin, M.N., Daud, W.W., Abbas, H.F., 2013. Potential hydrogen and non-condensable gases production from biomass pyrolysis: insights into the process variables. Renew. Sust. Energy Rev. 27, 204-224.
- [55] Wang, P., Zhang, J., Shao, Q., Wang, G., 2018. Physicochemical properties evolution of chars from palm kernel shell pyrolysis. J. Therm. Anal. Calorim. 133(3), 1271-1280.
- [56] Wang, Q., Zhang, X., Sun, S., Wang, Z., Cui, D., 2020. Effect of CaO on pyrolysis products and reaction mechanisms of a corn stover. ACS Omega. 5(18), 10276-10287.
- [57] White, J.E., Catallo, W.J., Legendre, B.L., 2011. Biomass pyrolysis kinetics: a comparative critical review with relevant agricultural residue case studies. J. Anal. Appl. Pyrolysis. 91(1), 1-33.
- [58] Yargicoglu, E.N., Sadasivam, B.Y., Reddy, K.R., Spokas, K., 2015. Physical and chemical characterization of waste wood derived biochars. Waste Manage. 36, 256-268.
- [59] Yi, Q., Qi, F., Cheng, G., Zhang, Y., Xiao, B., Hu, Z., Liu, S., Cai, H., Xu, S., 2013. Thermogravimetric analysis of co-combustion of biomass and biochar. J. Therm. Anal. Calorim. 112(3), 1475-1479.
- [60] Yuan, X., Ding, X., Leng, L., Li, H., Shao, J., Qian, Y., Huang, H., Chen, X., Zeng, G., 2018. Applications of bio-oil-based emulsions in a DI diesel engine: the effects of bio-oil compositions on engine performance and emissions. Energy. 154, 110-118.
- [61] Zaman, C.Z., Pal, K., Yehye, W.A., Sagadevan, S., Shah, S.T., Adebisi, G.A., Marlina, E., Rafique, R.F., Johan, R.B., 2017. Pyrolysis: a sustainable way to generate energy from waste. Rijeka, Croatia: IntechOpen. BoD-Books on Demand. 1, 316806.
- [62] Zhang, Q., Chang, J., Wang, T., Xu, Y., 2007. Review of biomass pyrolysis oil properties and upgrading research. Energy Convers. Manage. 48(1), 87-92.



**Dr. Ranjeet Kumar Mishra** is an Assistant Professor at the Department of Chemical Engineering, M.S. Ramaiah Institute of Technology, Bangalore, India. Dr. Mishra received his Ph.D. from the Indian Institute of Technology Guwahati (IITG) Assam in 2019. He has published more than 30 research articles in various peer-reviewed journals and holds an h-index of 16 with over 1300 citations. His current research interests are biomass conversion, pyrolysis, waste management, biochar, biofuel, nano-materials, bio-catalyst,

biodiesel, nanotechnology, hydrothermal liquefaction, etc. His Google Scholar profile can be found at the following link:

<https://scholar.google.com/citations?user=-GdsIWAAAAAJ&hl=en>



**Prof. Kaustubha Mohanty** is a Professor and Head of the Department of Chemical Engineering at the Indian Institute of Technology Guwahati, India. Prof. Mohanty also served as Head of the School of Energy Science and Engineering at IITG. He has authored/co-authored 3 books and 20 book chapters, published more than 170 research articles in peer-reviewed international journals, and holds an h-index of 46 with over 7000 citations. His current research interests are biofuels, biomass pyrolysis, biological wastewater treatment, heterogeneous catalysis, microalgae biorefinery, membrane-based separation, and waste management. His Google Scholar profile can be found at the following link:

<https://scholar.google.co.in/citations?user=QOFTgxAAAAAJ&hl=en>